Journal of Architectural and Planning Research
37:4 (Winter, 2023) 43

INTERACTION EFFECTS AND THRESHOLD RESPONSES OF COARSE AND FINE RECYCLED AGGREGATE REPLACEMENT IN GEOPOLYMER MASONRY PRISMS

P. Healey

The mechanical response of sustainable masonry assemblages depends not only on the absolute strengths of their constituent units and mortars, but also on how coarse- and fine-recycled aggregate substitutions alter the coupled unit–mortar system. This study presents a design-space reanalysis of a ten-mix experimental matrix of cement and geopolymer masonry prisms tested in compression, flexural bond, and shear bond. A stage-wise framework isolates four effects: binder substitution, mortar-class upgrade, RCA-only replacement, and the incremental penalty of adding RFA after full RCA replacement. Three derived indicators are used: performance retention, replacement-stage sensitivity, and mortar amplification. All reported percentages were recalculated directly from the mix-level dataset, and the resulting trends are interpreted as matrix-specific rather than as formal statistical interactions. Within this dataset, prism compressive strength is most sensitive to coarse aggregate replacement, with a 43.3 % *loss under RCA-only substitution and a further* 18.4 % *loss when RFA is added at fixed RCA100. Flexural bond is sensitive to both stages, dropping by* 34.3 % *under RCA-only replacement and by another* 32.8 % *when RFA is introduced. Shear bond behaves differently: it increases by about* 29.7 % *under RCA-only replacement and changes only marginally when RFA is added. Along the equal-replacement path, the most severe flexural-bond loss occurs already at 25% combined replacement, whereas shear bond recovers beyond 50% replacement. Compression failure modes shift from conical break to cone-and-split and then to cone-and-shear as combined replacement increases, while stronger mortars promote face-shell separation. The revised interpretation provides cautious design-oriented guidance for compression-dominated, flexure-sensitive, and shear-sensitive masonry applications within the scope of the studied system.*

https://doi.org/10.66033/japr2022-404

INTRODUCTION

Decarbonizing masonry construction requires simultaneous reductions in Portland-cement consumption and virgin-aggregate extraction. Geopolymer binders and recycled aggregates therefore represent an attractive pairing: the former can reduce clinker demand, while the latter valorize construction and demolition waste and relieve pressure on natural aggregate resources (Abuowda et al., 2022; Chen et al., 2018; Golewski, 2020; Najm et al., 2021). In masonry, however, the key design question is how substitutions introduced in units and mortars reshape assemblage response. RCA influences the block-scale load path through the masonry unit, whereas RFA changes mortar rheology, water retention, interfacial filling, and bond development (Corinaldesi, 2009; Moriconi et al., 2003; Murthi et al., 2022; Saba & Assaad, 2021). Consequently, the structural significance of recycled-aggregate replacement cannot be inferred from unit or mortar strength alone.

Recent studies have shown that geopolymer masonry can achieve competitive compressive capacity and, in several cases, superior bond performance relative to cement-based systems (Kumble et al., 2023; Singh et al., 2020). Studies on recycled-aggregate masonry have also reported reductions in prism compression together with response-specific changes in crack development and interface behavior (Guo et al., 2018; Nayaka et al., 2021; Sadek & El-Attar, 2015). What remains insufficiently resolved is how coarse and fine substitutions should be interpreted when they are introduced together: whether they penalize the same response channels, whether one stage dominates another, and whether apparent inflection points reflect meaningful transitions or only isolated mix differences.

A recent experimental campaign on geopolymer masonry prisms incorporating RCA in geopolymer concrete masonry units and RFA in geopolymer mortars provides a suitable basis for addressing these questions (Abuowda et al., 2022). That study showed that geopolymer prisms retained compressive strength comparable to cement benchmarks while attaining much higher flexural and shear bond strengths, that increasing replacement reduced prism compressive strength and flexural bond but not shear bond in the same manner, and that mortar strength affected bond more than compression while failure modes shifted toward more shear-dominated cracking (Abuowda et al., 2022). Because the design space was interpreted mainly through direct mix comparisons and constituent-strength correlations, a stage-wise reanalysis is needed to separate the roles of binder type, mortar class, RCA substitution in units, and RFA substitution in mortar.

The present study addresses that gap through a focused reanalysis of the same ten-mix experimental matrix. Rather than asking which mix performed best, the study asks how the performance landscape changes when coarse and fine recycled aggregate substitutions are decomposed into distinct stages and interpreted as coupled system responses. Four hypotheses are examined:

- **H1:** prism compressive strength is dominated by coarse replacement in the masonry unit and is substantially less sensitive to the subsequent addition of recycled fines in the mortar;
- **H2:** flexural bond is penalized by both stages of replacement and is therefore more interaction-sensitive than prism compression;
- **H3:** shear bond exhibits non-monotonic behavior, with early disruption at low combined replacement followed by recovery once the interface benefits of rougher recycled aggregates become dominant; and
- **H4:** upgrading the mortar from S- to M-type enhances bond responses much more than prism compression, especially when unit strength has already been reduced by RCA replacement.

These hypotheses are tested using a transparent reanalysis framework built on directly reported mix properties and prism responses. Because the available evidence is mix based rather than specimen resolved, the objective is to extract internally consistent effect rankings and threshold-like trends from the design space rather than to fit a formal statistical interaction model. The revised manuscript accepts a ranking only when it remains consistent with the original experimental observations and with established masonry response patterns reported in the literature. The resulting manuscript quantifies the response-specific sensitivity of compressive, flexural-bond, and shear-bond performance to RCA and RFA in separate stages, identifies inflection-like transitions in response evolution and compression failure mode along the equal-replacement path, and translates those findings into application-oriented guidance explicitly limited to the analyzed matrix.

EXPERIMENTAL BASIS AND REANALYSIS FRAMEWORK

Source experimental matrix

The reanalysis is grounded in the ten-mix masonry-prism program reported by Abuowda et al. (Abuowda et al., 2022). That program included two cement-based benchmark prisms made with natural aggregates and eight geopolymer prisms in which RCA was incorporated in concrete masonry units and RFA in masonry mortars. Prism responses were measured at 28 days under ASTM C1314 compression, ASTM E518 flexural bond, and EN 1052-3 shear bond. The design matrix also varied mortar class (S or M), allowing the effect of mortar strength to be evaluated separately from aggregate replacement (Abuowda et al., 2022).

For the purposes of the present analysis, all tabulated values of unit strength, mortar strength, prism compressive strength, flexural bond strength, and shear bond strength were transcribed directly. When a quantity was shown graphically but not listed numerically in the main text, it was digitized from the original plot and rounded to two decimal places. Every reported percentage change, sensitivity, and retention value in the present manuscript was then recalculated from the dataset in Table 1. The recalculated values were checked against the qualitative rankings and failure descriptions reported in the source article, and mechanistic explanations were retained only when they were also compatible with prior masonry studies cited in the Discussion. This procedure improves transparency and internal consistency, but it remains a comparative reanalysis and does not replace the original specimen-level measurements reported by the experimental study.

Reanalysis dataset

Table 1 summarizes the mix-level dataset used here. The notation follows the original experimental campaign: `CM` denotes cement-based prisms, `GM` denotes geopolymer prisms, `RCA` is the replacement percentage of coarse aggregate in masonry units, `RFA` is the replacement percentage of fine aggregate in mortar, and `S/M` indicate ASTM mortar classes.

Table 1: Mix-level dataset used in the interaction reanalysis.

Mix ID	Geo.	M-type	RCA (%)	RFA (%)	f_b (MPa)	f_m (MPa)	f_c (MPa)	f_r (MPa)	f_v (MPa)
CM-RCA0-S-RFA0	0	0	0	0	44.0	20.7	42.5	0.33	0.22
CM-RCA0-M-RFA0[a]	0	1	0	0	44.0	33.2	43.6	0.58	0.37
GM-RCA0-S-RFA0	1	0	0	0	40.0	16.0	43.0	1.02	0.37
GM-RCA0-M-RFA0	1	1	0	0	40.0	23.7	45.3	1.30	1.02
GM-RCA25-S-RFA25[a]	1	0	25	25	37.2	15.0	33.5	0.32	0.32
GM-RCA50-S-RFA50[a]	1	0	50	50	33.0	14.7	28.0	0.64	0.41
GM-RCA75-S-RFA75[a]	1	0	75	75	29.2	14.7	26.7	0.52	0.46
GM-RCA100-S-RFA100	1	0	100	100	24.9	14.5	19.9	0.45	0.46
GM-RCA100-S-RFA0	1	0	100	0	24.9	16.0	24.4	0.67	0.48
GM-RCA100-M-RFA0[a]	1	1	100	0	24.9	23.7	25.6	1.09	1.01

[a] Prism-level values digitized from the original figures where not explicitly reported in the narrative text of the experimental study.

Derived indicators

To distinguish the roles of coarse and fine recycled aggregates, three derived indicators were introduced.

First, a *performance-retention index* was defined for each response $y \in \{f_c, f_r, f_v\}$ relative to the natural-aggregate geopolymer baseline with S-type mortar:

$$R_y = \frac{y_i}{y_{\text{GM-RCA0-S-RFA0}}}. \tag{1}$$

Second, *replacement-stage sensitivities* were computed to separate the effect of coarse substitution from the incremental effect of recycled fines:

$$S_y^{\text{RCA}} = \frac{y_{(100,0,S)} - y_{(0,0,S)}}{100}, \qquad S_y^{\text{RFA}} = \frac{y_{(100,100,S)} - y_{(100,0,S)}}{100}. \tag{2}$$

Here, S_y^{RCA} measures the response change per percentage point of RCA when RFA is held at 0%, while S_y^{RFA} measures the incremental change per percentage point of RFA after unit replacement has already reached RCA100.

Third, a *mortar amplification index* was defined to quantify the benefit of upgrading from S- to M-type mortar:

$$A_y^{M/S} = \left(\frac{y_M - y_S}{y_S}\right) \times 100\%. \tag{3}$$

These indicators were evaluated under four comparison families: (i) cement versus geopolymer at 0% recycled aggregates, (ii) S- versus M-type mortar at fixed aggregate state, (iii) RCA-only replacement, and (iv) equal RCA/RFA replacement along the combined path 0%, 25%, 50%, 75%, and 100%. In the present manuscript, the term *interaction* is used in an engineering sense to denote coupled response changes across the unit–mortar assemblage under staged substitution. It does not imply estimation of a formal factorial interaction coefficient, since the source program is not a replicated full-factorial design. Accordingly, the quantitative results below are best read as design-space effect magnitudes within the studied matrix, and any threshold-like language refers to inflection features observed in this dataset rather than universal critical values.

Failure-mode interpretation

The original compression failure classifications were reinterpreted as an auxiliary marker of system-level behavioral change rather than as a standalone proof of a discrete threshold. The relevant sequence reported by Abuowda et al. (Abuowda et al., 2022) is: conical break at 0% combined replacement, cone-and-split at 25–50%, and cone-and-shear at 75–100%. When stronger mortars were used without RFA, the governing failure mode shifted instead to face-shell separation, indicating a transfer of weakness from the joint toward the masonry unit. In the present reanalysis, these classifications are used to corroborate the response trends, not to substitute for statistical evidence.

RESULTS

Binder substitution and mortar-class effects

At natural aggregate condition, replacing cement with a geopolymer binder caused only negligible changes in prism compressive strength but very large improvements in bond. For S-type mortar, f_c increased from 42.5 MPa to 43.0 MPa (1.2 %), while f_r increased from 0.33 MPa to 1.02 MPa (209 %) and f_v increased from 0.22 MPa to 0.37 MPa (68 %). For M-type mortar, the same comparison produced a modest 3.9 % increase in f_c, alongside gains of 124 % in f_r and 176 % in f_v. These recalculated effect sizes are fully consistent with the original study's qualitative conclusion that geopolymerization affected bond much more strongly than prism compression (Abuowda et al., 2022). In the present reanalysis, binder substitution is therefore interpreted mainly as an interface-level benefit rather than as a direct increase in unit–mortar compressive capacity.

Mortar upgrading from S- to M-type had a comparatively small influence on prism compression but a strong influence on bond, especially in the geopolymer system. Under natural aggregates, the M-type mortar increased f_c by only 5.3 %, but increased f_r by 27.5 % and f_v by 175.7 %. At RCA100 with RFA0, the same mortar upgrade again changed f_c only marginally (4.9 %), while increasing f_r by 62.7 % and f_v by 110.4 %. The amplification is therefore concentrated in the bond-governed responses, not in prism compression.

Stage-wise roles of coarse and fine recycled aggregate replacement

Figure 1 shows the stage-wise response changes. RCA-only replacement from GM-RCA0-S-RFA0 to GM-RCA100-S-RFA0 caused the largest penalty in prism compression, reducing f_c by 43.3 %. The corresponding changes in bond were milder for flexure (−34.3 %) and opposite in sign for shear, which improved by 29.7 %. Once unit replacement had already reached 100% RCA, adding RFA to the mortar from 0% to 100% caused an additional 18.4 % reduction in f_c and a 32.8 % reduction in f_r, while changing f_v by only −4.2 %. The stage ranking therefore supports the view that different response channels are affected differently even when the total replacement level is nominally the same.

These stage-wise comparisons reveal a clear response hierarchy. Compression is much more coarse-sensitive than fine-sensitive:

$$|S_{f_c}^{\mathrm{RCA}}| = 0.186 \text{ MPa per percentage point} \quad \text{versus} \quad |S_{f_c}^{\mathrm{RFA}}| = 0.045 \text{ MPa per percentage point.}$$

The ratio exceeds 4, indicating that the masonry-unit replacement stage dominates axial load-path degradation. Flexural bond is sensitive to both stages:

$$|S_{f_r}^{\mathrm{RCA}}| = 0.0035 \text{ MPa per percentage point}, \qquad |S_{f_r}^{\mathrm{RFA}}| = 0.0022 \text{ MPa per percentage point},$$

which supports the interpretation that flexural bond depends on both block integrity and mortar-side interface quality. Shear bond shows the most distinctive stage decomposition:

$$S_{f_v}^{\mathrm{RCA}} = +0.0011 \text{ MPa per percentage point}, \qquad S_{f_v}^{\mathrm{RFA}} = -0.0002 \text{ MPa per percentage point}.$$

Thus, RCA replacement is associated with a net improvement in shear transfer, while added RFA at fixed RCA100 is essentially neutral. These rankings are derived directly from the reported mix values rather than from curve fitting, and they remain consistent with the source study's observation that shear bond did not deteriorate in the same way as compression and flexural bond (Abuowda et al., 2022).

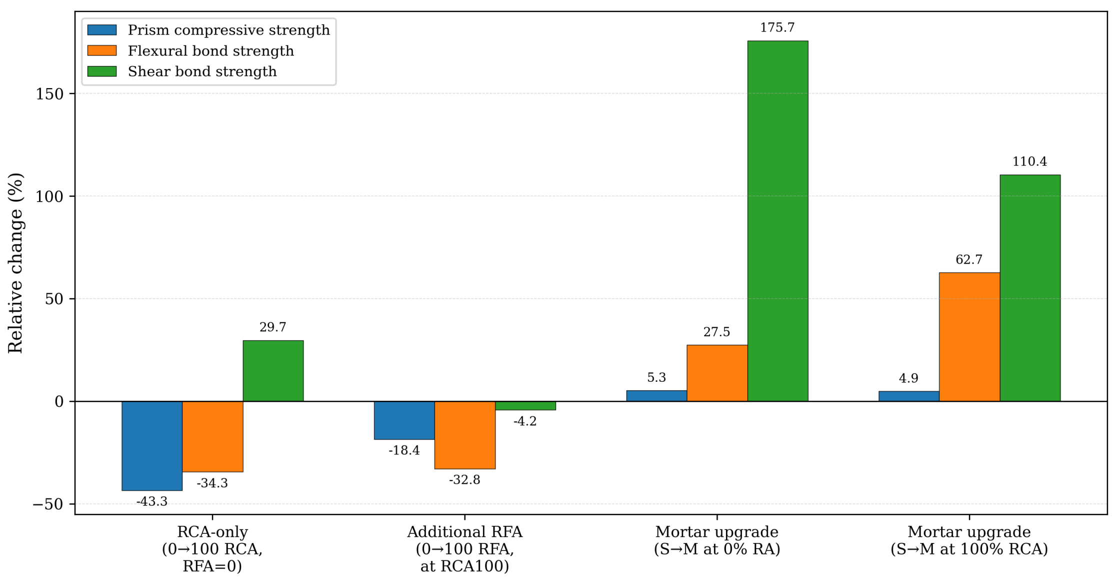

Figure 1: Stage-wise response changes for prism compression, flexural bond, and shear bond. The figure separates the effects of RCA-only replacement, the additional penalty caused by introducing RFA after RCA100, and the amplification caused by upgrading the mortar from S- to M-type.

Combined RCA/RFA path and threshold behavior

The equal-replacement path reveals pronounced nonlinearity (Figure 2). Prism compressive strength decreases monotonically from the natural-aggregate geopolymer baseline, but the rate of decline is not uniform. The largest drop occurs immediately between 0% and 25% replacement (−9.5 MPa), followed by a smaller drop to 50% replacement (−5.5 MPa), a temporary flattening between 50% and 75% replacement (−1.3 MPa), and then another large drop between 75% and 100% replacement (−6.8 MPa). Within this matrix, the pattern is more consistent with an inflection-like change in deterioration rate than with a sharp threshold.

Flexural bond exhibits even stronger non-monotonicity. The response falls from 1.02 MPa at 0% replacement to 0.32 MPa at 25%, which is already the minimum value along the entire combined path. It then recovers to 0.64 MPa at 50%, before declining gradually to 0.45 MPa at 100%. In retention terms, the 25% mix preserves only 31% of the natural-aggregate geopolymer flexural-bond capacity, whereas the 50% and 75% mixes preserve 63% and 51%, respectively. The early minimum indicates that low-level simultaneous substitution can disrupt bond continuity before roughness- and water-retention-related benefits of the recycled system begin to offset part of the loss. The original experimental study also identified the GM-RCA25-S-RFA25 mixture as the weakest bond-performing geopolymer mix and associated this behavior with inferior RFA gradation (Abuowda et al., 2022).

Shear bond follows a U-shaped trend. The response decreases slightly from 0.37 MPa at 0% replacement to 0.32 MPa at 25%, then recovers to 0.41 MPa at 50% and reaches 0.46 MPa at 75–100%. From 50% onward, shear performance exceeds the natural-aggregate geopolymer baseline. This trend should be interpreted cautiously, but it is consistent with the view that interfacial roughness and mechanical interlock associated with recycled aggregates can partly compensate for losses visible in unit and mortar compression.

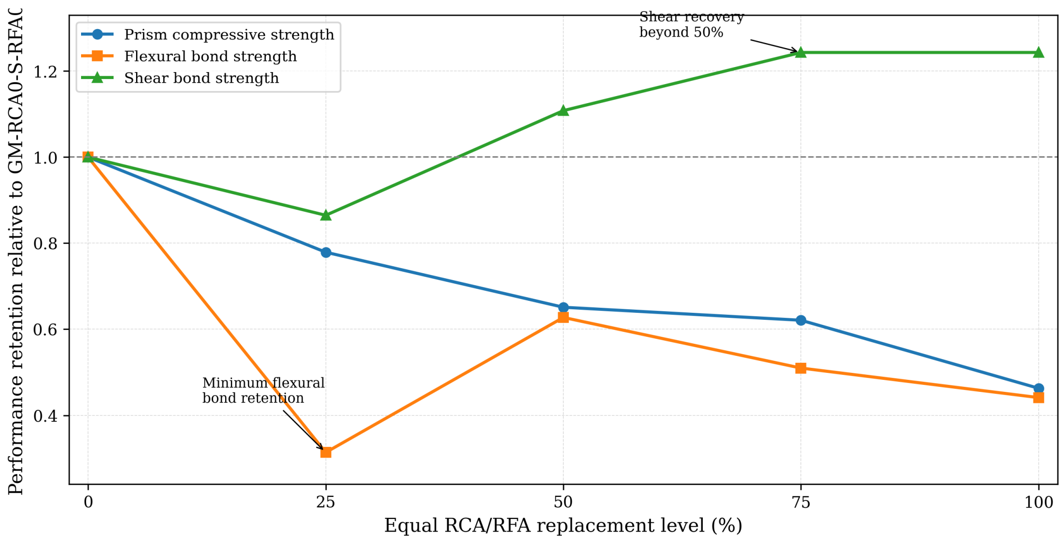

Figure 2: Performance retention along the equal RCA/RFA replacement path, normalized by the natural-aggregate geopolymer prism with S-type mortar. Compression degrades monotonically, flexural bond reaches an early minimum at 25%, and shear bond recovers beyond 50% replacement.

Failure-mode transition under compression

The threshold-like character of the combined path is reinforced by the compression failure sequence shown in Figure 3. At 0% combined replacement, the prism failed by conical break. At 25% and 50% replacement, the mode changed to cone-and-split, indicating intensified tensile splitting within the unit. At 75% and 100% combined replacement, the mode became cone-and-shear, signaling a more pronounced shear-dominated crack trajectory. Taken together with the strength trend, this sequence supports the interpretation that the deterioration of the masonry unit and the joint changes the dominant failure mechanism once combined replacement exceeds about 50% within the studied matrix. Because the source data are not specimen resolved, this should be read as corroborative evidence of a regime shift rather than as proof of a universal threshold.

A different transition occurs when mortar strength is increased without introducing RFA. Both GM-RCA0-M-RFA0 and GM-RCA100-M-RFA0 failed by face-shell separation rather than by cone-and-shear. This indicates that higher bond capacity can transfer the critical state away from joint-controlled cracking toward unit-controlled tensile failure. In practical terms, mortar strengthening does not “fix” the system uniformly; instead, it relocates the governing weakness.

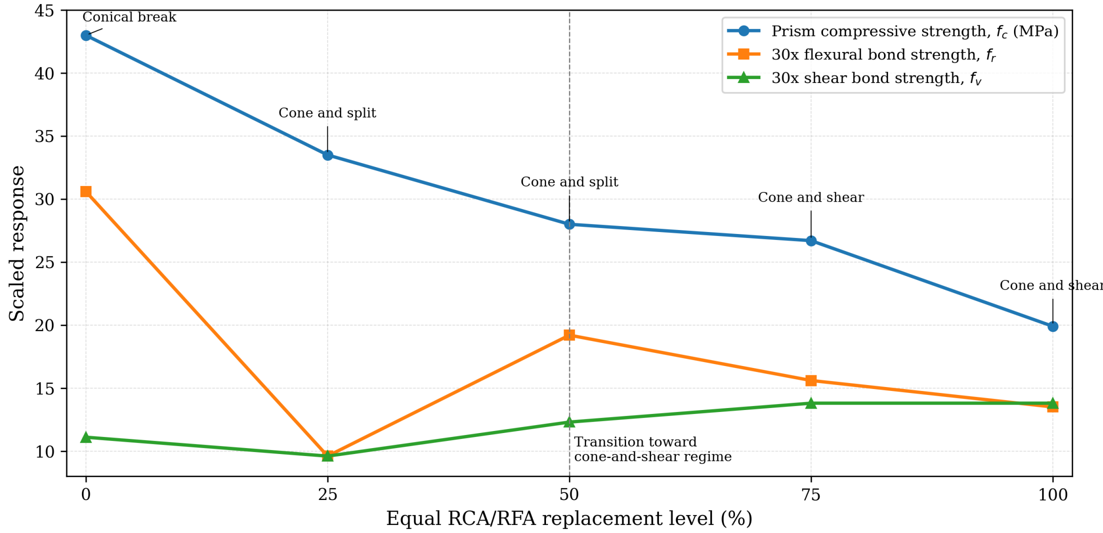

Figure 3: Response evolution and compression failure-mode transition along the equal RCA/RFA replacement path. Flexural and shear bond strengths are scaled for graphical comparison with prism compression. The failure sequence changes from conical break to cone-and-split and then to cone-and-shear as combined replacement increases.

Response-specific design implications

The reanalysis permits a clearer application-oriented interpretation than direct mix ranking alone. For compression-governed masonry, coarse replacement is the primary concern. The RCA-only stage accounts for the majority of the total compression loss, and combined replacement beyond 50% coincides with the cone-and-shear failure regime. For flexure-sensitive applications, the principal warning is different: the most severe bond penalty appears already at 25% combined replacement, meaning that low-to-moderate simultaneous replacement should not be assumed benign. For shear-sensitive applications, the ranking changes again. Once replacement exceeds 50%, the geopolymer prisms deliver shear bond at or above the natural-aggregate geopolymer baseline, and M-type mortar can raise f_v to approximately 1.0 MPa even with RCA100.

These findings imply that there is no single "optimal" replacement level independent of the governing structural demand. A mix suitable for compression design is not necessarily the best for bond-governed performance, and vice versa. The practical value of the reanalysis therefore lies in separating limit-state-specific replacement guidance rather than seeking one universal sustainable masonry recipe. Any design recommendation should therefore be understood as conditional on the source chemistry, aggregate quality, masonry geometry, and curing regime represented in the analyzed matrix.

DISCUSSION

Why coarse and fine replacements act differently

The contrasting stage sensitivities can be interpreted mechanistically. RCA replacement primarily alters the load-bearing skeleton of the masonry unit. Because prism compression is largely transmitted through the blocks, reductions in unit quality exert a first-order influence on f_c, consistent with studies showing that prism compression depends more strongly on block strength than on mortar strength (Henrique Nalon et al., 2020; Thaickavil & Thomas, 2018). Within this system, the coarse-aggregate substitution stage is more than four times as influential as the subsequent fine-aggregate stage in terms of compressive-strength sensitivity.

RFA affects the system differently. It modifies the mortar through surface area, angularity, water demand, and retention. These changes do not strongly determine prism compression once the unit has become the weak link, but they directly influence interface formation and therefore bond. The near-equal importance of RCA and RFA for flexural bond supports the concept that flexural failure mobilizes both unit-side integrity and mortar-side adherence (Rao et al., 1996; Taha & Shrive, 2001). The negligible incremental effect of RFA on shear bond at fixed RCA100 suggests that the beneficial interface roughness created by recycled materials may already be largely activated by the time full unit replacement is reached.

Interpretation of the non-monotonic bond trends

The early minimum in flexural and shear bond at 25% combined replacement is one of the most important outcomes of the present study. A monotonic interpretation of recycled-aggregate replacement would miss this behavior. The result suggests that partial substitution can initially destabilize grading, packing, and interfacial continuity before roughness-driven interlock develops at higher replacement levels. The original experimental study associated the weakest 25% mixture with poor RFA gradation, which aligns with this interpretation (Abuowda et al., 2022). The subsequent recovery of both f_r and f_v between 25% and 50% replacement is therefore more plausibly interpreted as a systems effect than as random fluctuation, although the present design cannot test that proposition statistically. The 25% point should therefore be interpreted as an inflection within this matrix, not as a universal critical replacement level.

This behavior matters because it shifts the framing from strength loss alone to mechanism change with replacement level.

Role of mortar strengthening

The mortar-class contrasts reveal another important asymmetry. Increasing mortar strength from S- to M-type produces only marginal gains in prism compression but very large increases in both flexural and shear bond. This is consistent with previous studies showing that stronger mortars do not proportionally increase prism compression once the unit controls the axial response, but they can markedly enhance bond by improving adhesion and interlock (Henrique Nalon et al., 2020; Javed et al., 2022; Reddy & Vyas, 2008). The present reanalysis shows that this upgrade remains effective even after severe coarse replacement. M-type geopolymer mortars therefore provide a practical way to recover bond performance when recycled coarse aggregate is used aggressively.

Implications for standards and future modelling

Current masonry design equations usually rely on constituent compressive strengths and therefore assume smooth monotonic behavior. The present results indicate that such formulations are insufficient when sustainable substitutions alter response channels in opposite directions. A practical design framework for geopolymer recycled-aggregate masonry should therefore distinguish at least three behavioral regimes within the tested system:

(i) compression-controlled mixtures, governed mainly by unit-side coarse replacement;

(ii) flexure-controlled mixtures, governed by both coarse replacement and mortar-side interface quality; and

(iii) shear-controlled mixtures, in which recycled-aggregate roughness and water retention may partly offset strength losses.

This regime-based interpretation provides a clearer basis for future constitutive modelling and masonry specifications. Future calibration should include specimen-level variability, interfacial characterization, and independent datasets.

LIMITATIONS

Several limitations should be acknowledged. First, the reanalysis operates at mix level and therefore cannot reproduce specimen-level variance structure, statistical significance, or within-mix scatter beyond what was reported in the original study. Second, a small subset of prism values had to be digitized from plots because the main text did not tabulate every numerical result; those points introduce additional uncertainty even though the principal effect rankings are larger than the digitization resolution. Third, the source matrix is not a replicated full-factorial experiment, so interaction is used here in a design-space sense rather than as a formal ANOVA coefficient. Fourth, the dataset represents one geopolymer chemistry, one aggregate source, one curing regime, and one masonry geometry, and the present paper adds no new microstructural, durability, or specimen-level statistical measurements. The findings are therefore strongest as a transparent reinterpretation of this matrix. External validation is still needed across alternative activator systems, block geometries, aggregate gradations, curing conditions, and durability exposures.

CONCLUSIONS

A design-space reanalysis of geopolymer masonry prisms incorporating recycled coarse and fine aggregates led to the following conclusions within the analyzed experimental matrix:

1. Prism compressive strength is most sensitive to the coarse-aggregate replacement stage in the masonry unit. RCA-only substitution caused a 43.3 % reduction in f_c, whereas adding RFA after RCA100 caused a further 18.4 % decrease.

2. Flexural bond is sensitive to both replacement stages. RCA-only replacement reduced f_r by 34.3 %, and the addition of RFA at fixed RCA100 caused a further 32.8 % reduction.

3. Shear bond follows a different response pattern from compression and flexural bond. RCA-only replacement improved f_v by about 29.7 %, and the subsequent addition of RFA caused only a negligible change.

4. Along the equal RCA/RFA path, the lowest flexural bond occurred already at 25% combined replacement, after which partial recovery was observed. Shear bond also reached an early minimum and then recovered to exceed the natural-aggregate geopolymer baseline beyond 50% replacement.

5. Compression failure modes changed from conical break to cone-and-split and then to cone-and-shear as combined replacement increased, which corroborates an inflection-like shift in the governing crack mechanism for this matrix.

6. Upgrading the mortar from S- to M-type had only a minor effect on prism compression but strongly amplified bond performance, especially shear bond. Within the analyzed system, this makes M-type geopolymer mortar a practical strategy for recovering interface performance in high-RCA masonry.

Overall, the results show that coarse and fine recycled aggregate substitutions do not affect geopolymer masonry through a single monotonic penalty. Instead, they act through different response channels and produce matrix-specific inflection behavior that should be interpreted with reference to the governing structural demand and the scope of the supporting experimental evidence.

DATA AVAILABILITY

All analyzed values were transcribed or digitized from the experimental matrix reported by Abuowda et al. (Abuowda et al., 2022). The original study states that the underlying data are available on request from the corresponding authors.

CONFLICT OF INTEREST

The author declares no conflict of interest.

REFERENCES

Abuowda, Y., Costa, J. R., Mestre, A., Miranda, M. S., Ferreira, F. H., & Costa, J. (2022). A case of late diagnosis of latent autoimmune diabetes in adults. *Cureus*, *14*(2).

Chen, Z., Li, J.-S., Zhan, B.-J., Sharma, U., & Poon, C. S. (2018). Compressive strength and microstructural properties of dry-mixed geopolymer pastes synthesized from ggbs and sewage sludge ash. *Construction and Building Materials*, *182*, 597–607. https://doi.org/10.1016/j.conbuildmat.2018.06.159

Corinaldesi, V. (2009). Mechanical behavior of masonry assemblages manufactured with recycled-aggregate mortars. *Cement and Concrete Composites*, *31*, 505–510. https://doi.org/10.1016/j.cemconcomp.2009.05.003

Golewski, G. L. (2020). Energy savings associated with the use of fly ash and nanoadditives in the cement composition. *Energies*, *13*, 2184. https://doi.org/10.3390/en13092184

Guo, Z., Tu, A., Chen, C., & Lehman, D. E. (2018). Mechanical properties, durability, and life-cycle assessment of concrete building blocks incorporating recycled concrete aggregates. *Journal of Cleaner Production*, *199*, 136–149. https://doi.org/10.1016/j.jclepro.2018.07.069

Henrique Nalon, G., Santos, C. F. R., Pedroti, L. G., Ribeiro, J. C. L., Verissimo, G. D. S., & Ferreira, F. A. (2020). Strength and failure mechanisms of masonry prisms under compression, flexure and shear: Components' mechanical properties as design constraints. *Journal of Building Engineering*, *28*, 101038. https://doi.org/10.1016/j.jobe.2019.101038

Javed, T., I, I., Singhal, R. K., Shabbir, R., Shah, A. N., Kumar, P., Jinger, D., Dharmappa, P. M., Shad, M. A., Saha, D., et al. (2022). Recent advances in agronomic and physio-molecular approaches for improving nitrogen use efficiency in crop plants. *Frontiers in Plant Science*, *13*, 877544.

Kumble, P., Prashant, S., & Achar, N. (2023). Bond strength of alkali-activated flyash based masonry system for sustainable construction. *SN Applied Sciences*, *5*, 360. https://doi.org/10.1007/s42452-023-05555-w

Moriconi, G., Corinaldesi, V., & Antonucci, R. (2003). Environmentally-friendly mortars: A way to improve bond between mortar and brick. *Materials and Structures*, *36*, 702–708. https://doi.org/10.1007/BF02479505

Murthi, P., Krishnamoorthi, S., Poongodi, K., & Saravanan, R. (2022). Development of green masonry mortar using fine recycled aggregate based on the shear bond strength of brick masonry. *Materials Today: Proceedings*, *61*, 413–419. https://doi.org/10.1016/j.matpr.2021.10.501

Najm, O., El-Hassan, H., & El-Dieb, A. (2021). Ladle slag characteristics and use in mortar and concrete: A comprehensive review. *Journal of Cleaner Production*, *288*, 125584. https://doi.org/10.1016/j.jclepro.2020.125584

Nayaka, R. R., Alengaram, U. J., Jumaat, M. Z., Fonseca, F. S., & Banerjee, A. (2021). Structural performance of masonry prisms, wallettes and walls containing high volume of industrial by-products–sustainable housing perspective. *Construction and Building Materials*, *303*, 124439. https://doi.org/10.1016/j.conbuildmat.2021.124439

Rao, K. V. M., Reddy, B. V. V., & Jagadish, K. S. (1996). Flexural bond strength of masonry using various blocks and mortars. *Materials and Structures*, *29*, 119–124. https://doi.org/10.1007/BF02486202

Reddy, B. V. V., & Vyas, C. V. U. (2008). Influence of shear bond strength on compressive strength and stress–strain characteristics of masonry. *Materials and Structures*, *41*, 1697–1712. https://doi.org/10.1617/s11527-008-9358-x

Saba, M., & Assaad, J. J. (2021). Effect of recycled fine aggregates on performance of geopolymer masonry mortars. *Construction and Building Materials*, *279*, 122461. https://doi.org/10.1016/j.conbuildmat.2021.122461

Sadek, D. M., & El-Attar, M. M. (2015). Structural behavior of rubberized masonry walls. *Journal of Cleaner Production*, *89*, 174–186. https://doi.org/10.1016/j.jclepro.2014.10.098

Singh, S., Aswath, M. U., & Ranganath, R. V. (2020). Performance assessment of bricks and prisms: Red mud based geopolymer composite. *Journal of Building Engineering*, *32*, 101462. https://doi.org/10.1016/j.jobe.2020.101462

Taha, M. M. R., & Shrive, N. G. (2001). The use of pozzolans to improve bond and bond strength. *Proceedings of the 9th Canadian Masonry Symposium*.

Thaickavil, N. N., & Thomas, J. (2018). Behaviour and strength assessment of masonry prisms. *Case Studies in Construction Materials*, *8*, 23–38. https://doi.org/10.1016/j.cscm.2017.12.007

AUTOBIOGRAPHICAL SKETCHES

Patsy Healey, Newcastle University, King's Gate, Newcastle upon Tyne, NE17RU, UK

Manuscript revisions completed 01 December 2023.